Monthly Notices of the ROYAL ASTRONOMICAL SOCIETY

MNRAS **495,** 4085–4097 (2020) doi:10.1093/mnras/staa1348
Advance Access publication 2020 May 15

Stability of Jovian Trojans and their collisional families

Timothy R. Holt ,[1,2]★ David Nesvorný,[2] Jonathan Horner,[1] Rachel King,[1] Raphael Marschall,[2] Melissa Kamrowski,[3] Brad Carter,[1] Leigh Brookshaw[1] and Christopher Tylor[1]

[1]*Centre for Astrophysics, University of Southern Queensland, Toowoomba, Queensland 4350, Australia*
[2]*Department of Space Studies, Southwest Research Institute, Boulder, CO 80302, USA*
[3]*Physics, University of Minnesota, Morris, MN 56267, USA*

Accepted 2020 May 7. Received 2020 May 5; in original form 2019 December 5

ABSTRACT

The Jovian Trojans are two swarms of objects located around the L_4 and L_5 Lagrange points. The population is thought to have been captured by Jupiter during the Solar system's youth. Within the swarms, six collisional families have been identified in previous work, with four in the L_4 swarm, and two in the L_5. Our aim is to investigate the stability of the two Trojan swarms, with a particular focus on these collisional families. We find that the members of Trojan swarms escape the population at a linear rate, with the primordial L_4 (23.35 per cent escape) and L_5 (24.89 per cent escape) population sizes likely 1.31 and 1.35 times larger than today. Given that the escape rates were approximately equal between the two Trojan swarms, our results do not explain the observed asymmetry between the two groups, suggesting that the numerical differences are primordial in nature, supporting previous studies. Upon leaving the Trojan population, the escaped objects move on to orbits that resemble those of the Centaur and short-period comet populations. Within the Trojan collisional families, the 1996 RJ and 2001 UV_{209} families are found to be dynamically stable over the lifetime of the Solar system, whilst the Hektor, Arkesilos and Ennomos families exhibit various degrees of instability. The larger Eurybates family shows 18.81 per cent of simulated members escaping the Trojan population. Unlike the L4 swarm, the escape rate from the Eurybates family is found to increase as a function of time, allowing an age estimation of approximately $1.045 \pm 0.364 \times 10^9$ yr.

Key words: methods: numerical – minor planets, asteroids: general.

1 INTRODUCTION

The Jovian Trojans are a population of small Solar system bodies comprising two swarms located around the leading (L_4) and trailing (L_5) Lagrange points of Jupiter. The larger and better known members of the Trojan swarms are named after the characters of the epic Greek poems that detail the Trojan war, The Iliad and The Odyssey (Homer 750 BC).

The Jovian Trojans were discovered in the early 20th Century, with the first (588 Achilles, Wolf 1907) being quickly followed by 617 Patroclus, 624 Hektor, and 659 Nestor (Heinrich 1907; Strömgren 1908; Ebell 1909; Kopff 1909). These objects were the first confirmation of a stable solution to the restricted three-body problem that had been proposed over a century earlier by Lagrange (1772).

At the time of writing, approximately 7200 objects have been discovered around the Lagrange points of Jupiter,[1] a number that is destined to rise still further in the coming years, as a result of the Rubin Observatory Legacy Survey of Space and Time (LSST), scheduled for first light in 2021 (Schwamb, Levison & Buie 2018b). Interestingly, the known Trojans are not evenly distributed between the two Trojan swarms. Instead, there is a marked asymmetry, with the leading L_4 swarm containing approximately 1.89 times the number of objects than the L_5 swarm. A number of studies have considered this asymmetry and have found it to be robust, a real feature of the population, rather than being the result of observational biases (Jewitt, Trujillo & Luu 2000; Nakamura & Yoshida 2008; Yoshida & Nakamura 2008; Vinogradova & Chernetenko 2015).

Although more than 7200 objects have been found in the region surrounding the Jovian Lagrange points, many of those objects may

★ E-mail: timothy.holt@usq.edu.au

[1]Taken from the JPL HORIZONS Solar System Dynamics Database https://ssd.jpl.nasa.gov/ (Giorgini et al. 1996), on 2019 November 13.

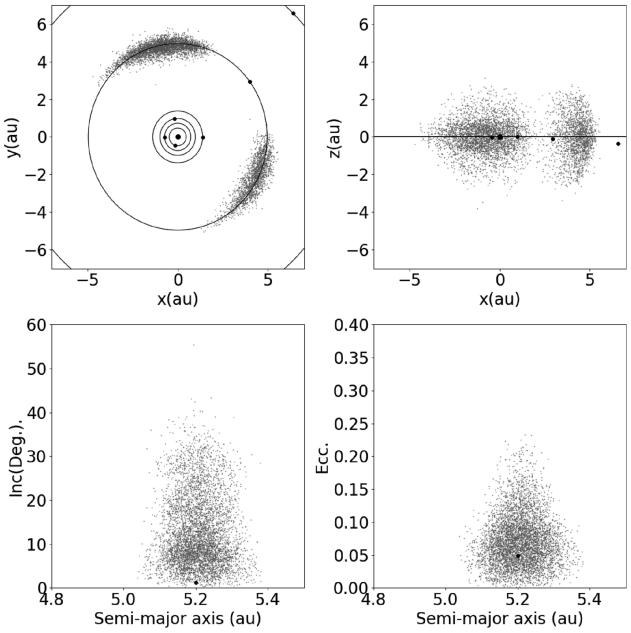

Figure 1. Distribution of 5553 Jovian Trojans for which proper elements have been generated (Knežević & Milani 2017). The top figures indicate the positions of the Trojans relative to the planets on 01-01-2000 00:00 in a face-on (*xy*; left) and edge-on (*xz*; right) orientation, in the ecliptic reference system. Bottom figures show the Trojans in osculating inclination (Inc.), eccentricity (Ecc), and semimajor axis space. Larger black dots indicate planets, with Jupiter being shown in the bottom diagrams. Data from NASA HORIZONS, as of 2019 August 19.

be temporarily captured objects, rather than permanent members of the Trojan population. Whilst the 'true' Trojans move on stable orbits that keep them librating around the L_4 and L_5 Lagrange points on billion year time-scales (e.g. Emery et al. 2015), temporarily captured objects would be expected to escape from the Trojan swarms on time-scales of thousands or tens of thousands of years. To confirm that a given object is truly a member of the Trojan population requires confirmation that the object's proper orbital elements (Milani & Knežević 1992) are stable, and that the object is truly trapped in 1:1 resonance with Jupiter. Simulations spanning more than 1×10^6 yr and transformation using Fourier transform analysis (Šidlichovský & Nesvorný 1996; Beaugé 2001; Brož & Rozehnal 2011) are used to devolve the osculations of potential Trojans to determine whether or not their orbits are truly resonant. The data base of those objects for which such analysis has been carried out can therefore be considered a set of contemporary stable Jovian Trojans, and includes 5553 numbered and multioppositional objects (Knežević & Milani 2017). Fig. 1 shows the current known configuration of the Jovian Trojan population.

In order to assess the observational completeness of the Trojan population, an examination of their size distribution is needed. The observed population of Jovian Trojans ranges in diameter from the largest, 624 Hektor, at ∼250 km (Marchis et al. 2014), down to objects several kilometres across (Emery et al. 2015). The size-frequency distribution for these objects is generally considered to be observationally complete to approximately 10 km in size (Grav et al. 2011; Emery et al. 2015), as shown in Fig. 2. The power law that best describes this size distribution is similar to that of the collisionally evolved Asteroid belt (Bottke et al. 2005). From this, it has been inferred that the Jovian Trojan population could contain as many as

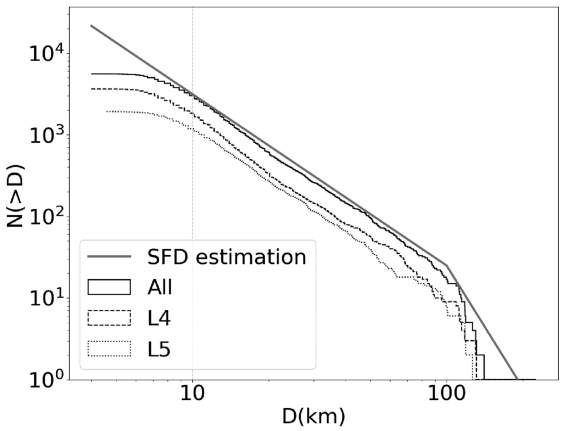

Figure 2. Cumulative size-frequency distribution of the Jovian Trojans. The solid line shows the distribution for the population as a whole, whilst the long-dash line shows the distribution among members of the leading L_4 swarm, and the dotted line shows the distribution for the trailing L_5 swarm. Data from NASA HORIZONS, as of 2019 August 19. Vertical grey, dashed line indicates observational completeness (Emery et al. 2015). The grey line shows the estimated complete size distribution (Nesvorný 2018).

a million objects greater than 1 km in diameter (Jewitt et al. 2000; Yoshida & Nakamura 2008; Yoshida & Terai 2017), though there are also indications that these may be optimistic estimates that grossly overestimate the true situation (e.g. Nakamura & Yoshida 2008).

1.1 The dynamics and origins of the Jovian Trojans

Due to their stability, it is thought that the Jovian Trojans date back to the early Solar system (e.g. Emery et al. 2015; Nesvorný 2018). Attempts to ascertain the origins of the Jovian Trojans need to explain their unique dynamical situation. As can be seen in Fig. 1, the population is dynamically 'warm', occupying two broad tori around the Lagrange points, with high orbital inclinations and eccentricities. An *in situ* formation would be expected to produce a 'cold' disc, with low orbital eccentricities and inclinations, reflective of the primordial protoplanetary disc. The mismatch between the observed population and the distribution that would be expected from *in situ* formation has led to the conclusion that the Jovian Trojans most likely did not form in their current orbits, but were in fact captured early in the Solar system's history (e.g. Morbidelli et al. 2005; Lykawka & Horner 2010; Nesvorný, Vokrouhlický & Morbidelli 2013; Pirani et al. 2019a).

One explanation for the observed orbital distribution of the Jovian Trojans comes in the form of the 'Nice' Model. This model invokes a period of chaotic disruption in the outer Solar system to explain the origin of the Late Heavy Bombardment (Tsiganis et al. 2005a; Morbidelli 2010; Levison et al. 2011; Nesvorný & Morbidelli 2012; Deienno et al. 2017; Nesvorný 2018), during which the Trojans were trapped in their current orbits from a population of dynamically unstable objects that were being scattered through the outer Solar system (Morbidelli et al. 2005; Lykawka & Horner 2010; Nesvorný et al. 2013). A recent attempt to explain the observed asymmetry, which is not explained by the 'Nice' model, proposes an alternative, that the Trojans were captured from the same region of the disc as Jupiter, and were transported during the planet's proposed inward migration (Pirani et al. 2019a). In an update to this *in situ* transport model, Pirani, Johansen & Mustill (2019b) explains the inclinations by invoking mixing in the Jovian feeding

region. These two competing theories for the origins of the Trojans highlight the importance of the population in our understanding of the early Solar system.

Previous long-term simulations of the Jovian Trojans (Levison, Shoemaker & Shoemaker 1997; Tsiganis, Varvoglis & Dvorak 2005b; Di Sisto, Ramos & Beaugé 2014; Di Sisto, Ramos & Gallardo 2019) have indicated that at least some of the members of both the L_4 and L_5 swarms are actually temporary captures, and will escape from the Trojan swarms on time-scales of $\sim 1 \times 10^6$ yr. The estimated fraction of Trojans that will escape the population on these time-scales varies somewhat between these studies, with Levison et al. (1997) proposing an escape rate of ∼12 per cent and Tsiganis et al. (2005b) estimating 17 per cent. More recent works, by Di Sisto et al. (2014, 2019), suggest a still higher escape rate, at 23 per cent for the L_4 and 28 per cent for the L_5 swarm. To some extent, the disparity among these results can be explained by the growth in the known Trojan population that occurred between one study and the next. Levison et al. (1997) considered a sample of only 178 numbered objects. In contrast, Tsiganis et al. (2005b) studied 246 numbered objects. The 2972 numbered Trojans that were simulated by Di Sisto et al. (2014, 2019) make it the largest previous study.

To further complicate the picture, detailed modelling of (1173) Anchises (Horner, Müller & Lykawka 2012) has shown that at least some of the unstable Jovian Trojans could still be primordial in nature. Indeed, that work, along with other studies in stability (Levison et al. 1997; Nesvorný et al. 2002c; Tsiganis et al. 2005b; Di Sisto et al. 2014, 2019), suggests that the original population of Jovian Trojans was larger than that observed today, and that it likely included objects with a range of stabilities. (1173) Anchises is stable on time-scales of hundreds of millions of years, and so might well be a representative of a once larger population of such objects, which have slowly escaped from the Trojan population since their formation. Following a similar argument, Lykawka & Horner (2010) propose a link between the Centaur population and the Jovian Trojans that escape, though this is disputed by Jewitt (2018) due to differences in the colour distributions of the two populations. Wong & Brown (2016) also use the observed colours of members of the Jovian Trojan population to propose a hypothesis for a common origin between the Trojans and the Edgeworth–Kuiper Belt objects. Such an origin is a good fit with the results of dynamical models that invoke an instability in the outer Solar system as the origin of the Jovian Trojans, in which the Jovian Trojans are captured from a similar source region to the Edgeworth–Kuiper Belt objects (Morbidelli et al. 2005; Nesvorný et al. 2013).

1.2 Collisional families amongst the Jovian Trojans

Elsewhere in the Solar system, other evolved populations contain dynamical families, the results of the collisional disruption of large parent bodies. Such collisional families have been identified in the asteroid main belt (see Hirayama 1918; Gradie et al. 1979; Zappala et al. 1984; Knežević & Milani 2003; Carruba et al. 2013; Milani et al. 2014; Nesvorný, Brož & Carruba 2015; Milani et al. 2017), the Hilda (Brož & Vokrouhlický 2008) and Hungaria (Warner et al. 2009; Milani et al. 2010) populations, the irregular satellites of the giant planets (Grav et al. 2003; Nesvorný et al. 2003; Sheppard & Jewitt 2003; Nesvorný, Beaug & Dones 2004; Grav & Bauer 2007; Jewitt & Haghighipour 2007; Turrini, Marzari & Beust 2008; Turrini, Marzari & Tosi 2009; Bottke et al. 2010; Holt et al. 2018) and the Haumea family in the Edgeworth–Kuiper belt (Brown et al. 2007; Levison et al. 2008; de la Fuente Marcos & de la Fuente Marcos 2018). The traditional methodology for identifying these families in small body populations was developed by Zappala et al. (1990, 1994) and is known as the Hierarchical Clustering Method (HCM) and utilizes distances in semimajor axis, eccentricity, and inclination parameter space to identify family members.

Table 1. Identified collisional families in the Jovian Trojan swarms, after Nesvorný et al. (2015).

Family	FIN	n	D_{LM} (km)	Tax.
L_4				
Hektor	1	12	225	D
Eurybates	2	218	63.88	C/P
1996 RJ	3	7	68.03	–
Arkesilaos	4	37	20.37	–
L_5				
Ennomos	5	30	91.43	–
2001 UV_{209}	6	13	16.25	–

Note. FIN: family identification number, used throughout this manuscript; n: number of family members; D_{LM}: diameter of the largest member; Tax.: identified taxonomic type (Bus 2002; Grav et al. 2012).

Historically, studies that attempted to identify such collisional families amongst the Jovian Trojans were limited by the number of objects that had been discovered at that time (Milani 1993). Additionally, as the Jovian Trojans librate around the Lagrange points, the calculation of proper elements used in family identification is problematic (Emery et al. 2015). For that reason, Beaugé (2001) used transformed proper elements to account for the librations present in the Jovian Trojan dynamics. As the number of known Jovian Trojans increased, additional dynamical clusters have been identified (e.g. Roig, Ribeiro & Gil-Hutton 2008; De Luise et al. 2010; Brož & Rozehnal 2011; Nesvorný et al. 2015; Vinogradova 2015; Rozehnal et al. 2016). Rozehnal et al. (2016) offer an expansion to the HCM developed by Zappala et al. (1990). This new 'randombox' method uses Monte Carlo simulations to determine the probability that the identified clusters are random in parameter space. Canonically, six collisional families, four in the L_4 swarm and two in the L_5, are now considered valid in the Jovian Trojan population (Nesvorný et al. 2015). Independent HCM analysis undertaken by Vinogradova (2015) has confirmed the four L_4 families, though they dispute the validity of the L_5 families. See Table 1 for details on the families we consider in this work.

Early imaging surveys suggest that there is a spectral commonality within the dynamical families (Fornasier et al. 2007) in the Jovian Trojans. More recent observational data have brought this into question (Roig et al. 2008), with a heterogeneity being seen in some unconfirmed families from the Sloan Digital Sky Survey (SDSS) colours. The confirmed Eurybytes and Hektor families, however, show a distinctive colour separation from the rest of the population (Roig et al. 2008; Brož & Rozehnal 2011; Rozehnal et al. 2016). Vinogradova (2015) also make comments on the taxonomy of the L4 families, based on SDSS taxonomy (Carvano et al. 2010). In these studies, the Eurybates family is found to consist mainly of C-types, and the Hektor family mostly D-types, under the Bus–Demeo taxonomy (Bus 2002; DeMeo et al. 2009).

Unlike collisional families in the asteroid belt, the determination of ages for the Trojan families remains elusive. Currently, there are two general methods used to determine family ages (Nesvorný et al. 2015). The first involves reverse integration n-body simulations of the identified family. A relatively young family, such as the Karin family (Nesvorný et al. 2002a), would show convergence in both longitude of ascending node and argument of pericentre as those simulations approach the time of the family's birth. However, such

simulations are not able to provide firm constraints on the ages of older families, as a result of the chaotic diffusion experienced by the members of those families over time. Once such diffusion has had sufficient time to act, reverse integration of family members will fail to show such convergence. A variation on this uses synthetic families to estimate the collisional family age (Milani & Farinella 1994; Nesvorný et al. 2002b). Some synthetic simulations by Brož & Rozehnal (2011) and Rozehnal et al. (2016) have calculated the age of the Hektor, Eurybates, and Ennomos families in the Trojan population, though these have relatively large, Gigayear ranges. In order to circumvent some of these issues, a second method of family age estimation was developed. This method relies on the modelling of asteroidal Yarkovsky drift (Vokrouhlický et al. 2006; Spoto, Milani & Knežević 2015; Bolin et al. 2017). The technique takes advantage of the fact that any collisional family will contain a large number of different sized objects, which would be expected to experience Yarkovsky drift (Bottke et al. 2006) at different rates. As a result, when the members of a collisional family are plotted in size, or its proxy absolute magnitude, versus orbital semimajor axis, they will form a characteristic 'V shape' (Vokrouhlický et al. 2006; Spoto et al. 2015; Paolicchi et al. 2019). The slope of the 'V' can then be used to estimate the age of the family. Using this method, a 4×10^9 yr old meta-family has been identified in the asteroid belt (Delbó et al. 2017). This method has been attempted with the Eurybates family (Milani et al. 2017), though due to the negligible Yarkovsky effect experienced by the Jovian Trojans, the age is unreasonably estimated at 1.4×10^{10} yr. This indicates that the method is inappropriate for age estimation of collisional families in the Jovian Trojan swarms.

1.3 This work

In this work, we utilize *n*-body simulations of the known Jovian Trojan population to consider the stability of previously identified collisional families (Nesvorný et al. 2015). This work considers 5553 numbered and multioppositional objects, a sample nearly double that of the previous largest study (Di Sisto et al. 2014, 2019), who considered 2972 numbered objects. By simulating the whole known population, we can include all identified collisional family members in the study. We divide this work into the following sections. Section 2 describes the methodology of the *n*-body simulations used as the basis for this work. We discuss the L_4 and L_5 swarms in Section 3. In Section 3.1, we use our simulations to study the rate at which objects escape from the Trojans, and discuss the implications of our results for the original size of the population, including the L_4/L_5 asymmetry and formation scenarios. We consider the stability of the collisional families in Section 4, with a particular focus on the large Eurybates family in Section 4.1.1. Concluding remarks are presented in Section 5.

2 METHODS

We selected the Jovian Trojan population for our simulations based on several criteria. An initial data set was obtained from the JPL Small-Body Database (Giorgini et al. 1996) by searching for and selecting all objects with orbital semimajor axes between 4.6 and 5.5 au and an orbital eccentricity less than 0.3. This process yielded an initial selection of 7202 objects, obtained on 2018 April 17. The ephemeris were retrieved from the NASA HORIZONS data base (Giorgini et al. 1996) for all objects using an initial time point of A.D. 2000-Jan-01 00:00:00.0000. We then filtered our sample to discard temporarily captured objects by limited selection to those objects present in the AstDys proper element data base (Knežević & Milani 2017). Since objects in this list require the completion of simulations spanning 1×10^6 yr to generate the proper elements of their orbits (Knežević & Milani 2017), this set can be considered initially stable objects. Once our sample was filtered in this way, we were left with a total of 5553 nominally 'stable' Trojans for this study, including 4780 numbered and 773 multioppositional objects.

In order to investigate the long-term dynamical evolution of the Jovian Trojan population, we carried out a suite of *n*-body integrations using the WFAST symplectic integrator within the *REBOUND* *n*-body dynamics package (Rein & Liu 2012; Rein & Tamayo 2015). Eight clones of each reference Trojan were created, distributed across the $\pm 1\sigma$ positional uncertainties from the HORIZONS data base (Giorgini et al. 1996). These eight 1σ clones were generated at the vertices of a cuboid in x–y–z space, with the reference particle in the centre. Therefore, in this work, we followed the evolution of a total of 49 977 collisionless, massless test particles in our simulations, nine particles for each of the 5553 Trojans. Our integrations modelled the evolution of our test particle swarms under the gravitational influence of the Sun and the four giant planets (Jupiter, Saturn, Uranus, and Neptune). Each individual simulation thus consisted of the Sun, four giant planets, the initial HORIZONS reference particle and the eight 1σ clones, with ephemeris in Solar system barycentric coordinates. All simulations were conducted on the University of Southern Queensland's High Performance Computing Cluster, Fawkes. We ran each simulation forward for 4.5×10^9 yr, with an integration time-step of 0.3954 yr, 1/30th of the orbital period of Jupiter (Barnes & Quinn 2004). The orbital elements of every test particle were recorded every 1×10^5 yr.

The Yarkovsky effect is a non-gravitational force that can act on small bodies (Bottke et al. 2006). The effect involves the asymmetric thermal radiation of photons from an object, which imparts a thrust on the object in question. This thrust will gradually change the semimajor axis of a body, with the scale and direction of the induced drift dependent on the thermal properties, axis of rotation and size of the object (Brož et al. 2005; Bottke et al. 2006). In the case of the Jovian Trojans, simulations of hypothetical objects have indicated that at small sizes (<1 km), the Yarkovsky effect could impact the stability of the objects (Wang & Hou 2017; Hellmich et al. 2019). As we are simulating known Jovian Trojans, the majority of the objects are greater than several kilometres in size (Emery et al. 2015), and have unknown or highly uncertain thermal properties (Slyusarev & Belskaya 2014; Sharkey et al. 2019). For these reasons, we have not included the Yarkovsky effect in our simulations.

3 ESCAPES FROM THE L4 AND L5 SWARMS

In each of our simulations, we track the position of a particle and record the time it escapes the Jovian Trojan population. A data base of the escape times of each particles is presented in the online supplementary material. We define these escapes as occurring once the test particle obtains an osculating semimajor axis of less than 4.6 au or greater than 5.5 au. In Table 2, we present the results of our simulations, showing the fraction of the total population that escaped from the Trojan population during our simulations. As part of our calculations, we include the volume of the object, as a proxy for mass. The density is only known for a single C-type Trojan, (617) Patroclus (Marchis et al. 2006). With the diversity of taxonomic types seen in even a small number of classified Trojans (Carvano et al. 2010; Grav et al. 2012; DeMeo & Carry 2013), using mass instead of volume could further propagate errors. The volumes were calculated from diameters in the HORIZONS data

Table 2. Escape percentages of Jovian Trojan swarm members.

	n	n_{test}	f_{EscR} (per cent)	f_{VEscR} (per cent)	f_{EscP} (per cent)	f_{VEscP} (per cent)	f_{Esc9C} (per cent)	f_{VEsc9C} (per cent)	$>10km f_{EscP}$ (per cent)	$>10km f_{VEscP}$ (per cent)
L_4	3634	32 706	22.23	22.97	23.19	23.35	5.01	7.36	23.28	23.37
L_5	1919	17 271	24.80	32.22	24.89	24.89	5.04	6.07	24.27	24.88
Total	5553	49 977	23.12	26.58	23.77	23.95	5.02	6.56	23.67	23.96

Note. n: Number of real Trojan members considered in the simulations; n_{test}: number of test particles simulated (eight clones, plus initial reference particle); f_{EscR}: numerical percentage of reference particles that escape; f_{VEscR}: volumetric percentage of reference particles that escape; f_{EscP}: numerical percentage Trojan particle pool, Reference and eight 1σ clones, that escape; f_{VEscP}: volumetric percentage Trojan particle pool, Reference and eight 1σ clones, that escape; f_{Esc9C}: numerical percentage Trojans where all nine particles escape; f_{VEsc9C}: volumetric percentage of Trojans where all nine particles escape; $>10km f_{EscP}$: numerical percentage of Trojan particle pool greater than 10 km that escape; $>10km f_{VEscP}$: volumetric percentage of Trojan particle pool greater than 10 km that escape.

base to a assumed sphere. Where diameters were unavailable, due to no recorded albedo, we made an estimate based on the H magnitude and mean geometric albedo (from NASA HORIZONS) of each Jovian Trojan swarm, following the methodology of Harris (1997). We use separate geometric albedos for the L4 (0.076) and L5 (0.071) swarms, as they are significantly different (Romanishin & Tegler 2018), though close to the mean geometric albedo (0.07) identified by Grav et al. (2011, 2012). There may be a size dependence on the albedos in the Trojan population (Fernández, Jewitt & Ziffer 2009; Grav et al. 2011, 2012), though only a relatively small number of objects have been studied in this way. In choosing to use consistent albedos, there may be some discrepancies between this work and future studies, as more robust albedos, diameters, and shape models are presented. We note that the observed L_4/L_5 asymmetry is lower when volume is considered (L_4 1.56 larger) than simply considering the number of known objects (L_4 1.89 larger).

The escape percentages of our reference particles are larger than the 12 per cent seen by Levison et al. (1997). In order to investigate this discrepancy, we consider the instability of the subset of the 178 Jovian Trojans known at the time of Levison et al. (1997). Using our simulations, we find an reference particle escape rate of 15 per cent, consistent with Levison et al. (1997) and similar to the 17 per cent found by Tsiganis et al. (2005b). Di Sisto et al. (2014, 2019) considered the 2972 numbered Trojans known at that time and found escape rates of 23 per cent and 28.3 per cent for the L_4 and L_5 swarms, respectively. The Di Sisto et al. (2014, 2019) results are closer to our escape rates for the reference particles, and the L_4 particle pool escapees. The escape percentages in the L_5 clone pool are lower in our simulations, closer to that of the L_4 swarm and the population as a whole.

The similar ratios in escape percentages between the two swarms confirm the findings of others (Nesvorný & Dones 2002; Tsiganis et al. 2005b; Nesvorný et al. 2013; Di Sisto et al. 2014, 2019), who argued that the observed Jovian Trojan swarm asymmetry cannot be the result of differences in the escape rate between the two Trojan swarms. The difference is therefore more likely due to differences in the number of objects that were initially captured to the swarms.

At first glance, the escape volume differences between the two swarms, shown in Table 2, could account for the asymmetry, particularly in terms of the reference particles (f_{VEscR} in Table 2). This can be explained by the escape of several large (<100 km diameter) reference objects. In the L_4 swarm, the reference particles of (1437) Diomedes and (659) Nestor escape the Trojan population. The reference particles of (3451) Mentor, (1867) Deiphobus, and (884) Priamus in the L_5 swarm also escape. (3451) Mentor and (659) Nestor are classified as X-type (Tholen 1984; Bus 2002). Once the 1σ clones are taken into account, f_{VEscP} in Table 2, this escape asymmetry in the volume is negated, resulting in near identical escape rates for the L_4 and L_5 swarms. This volumetric escape fraction (f_{VEscP} in Table 2) is very similar to the numerical escape fraction (f_{EscP} in Table 2) for the population and in each of the swarms. In order to further investigate the volumetric escapes, we can limit our selection to just objects for which the population can be considered to be observationally complete, those larger than 10 km (Emery et al. 2015). This reduces the numerical size of the population to 3003. When we repeat the analysis, the percentage of particles that escape only changes by fractions of a per cent in the population, as well as each swarm, see $>10km f_{EscP}$ and $>10km f_{VEscP}$ in Table 2. This additional analysis supports the hypothesis that the observed asymmetry between the swarms is due to implantation, rather than any volumetric differences.

We generate a conservative subset of the escape population, one where all nine particles of a given object escape. In this subset, f_{Esc9C} and f_{VEsc9C} in Table 2 escape percentages are much lower. These escapes represent the minimal set of escapes and show that the majority of the escaping population are statistically borderline. Those objects where all nine particles escape are deep into the parameter space identified as unstable by Levison et al. (1997) and Nesvorný et al. (2002c). With regards to the large Trojans, all particles of (1437) Diomedes escape the L_4 swarm by the end of our simulations.

The timing of the reference particle escapes are shown in Fig. 3. With larger changes in semimajor axis (Δa_p) and eccentricity (e_p), there is an increase in the instability. Proper inclination ($\sin - i_p$) appears to have little effect on the general instability of the particles. This general trend is consistent with other studies (Nesvorný & Dones 2002; Tsiganis et al. 2005b; Di Sisto et al. 2014, 2019). With the inclusion of the timing of escape, we show that there is a gradient to the instability trends, particularly in the Δa_p to e_p relationship. This is in a similar unstable parameter space to that identified in Nesvorný & Dones (2002).

3.1 Escape analysis

During our 4.5×10^9 yr simulations, we track the timing of any particles that escape the Jovian Trojan population. As the orbital elements of our test particles are recorded at intervals of 1×10^5 yr, the escape times are only accurate to that resolution. For this analysis, we pool our results for all test particles considered in this work, including the reference object and each of the eight 1σ clones, as independent objects. This gives statistical robustness to the analysis. A histogram of the escape percentages for the population as a whole, and each of the L_4 and L_5 swarms is presented in Fig. 4.

We create linear regression equations to the escape percentages as a function of time, independently for the combined population, and for the L_4/L_5 swarms. These equations along with their associated

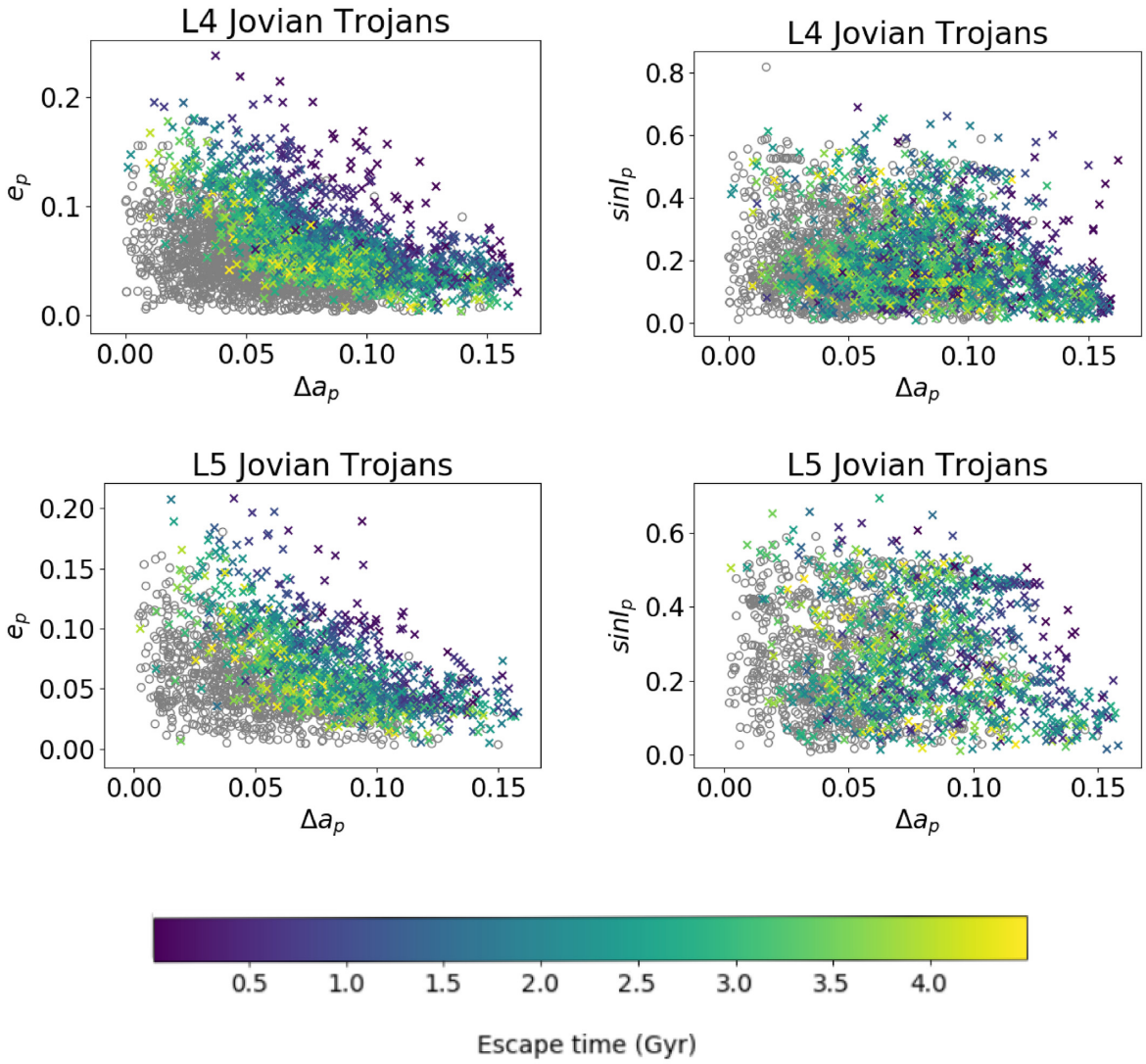

Figure 3. Escape analysis of Jovian Trojans in the L_4 and L_5 swarms simulated over 4.5 Gyr. Proper elements, semimajor axis (Δa_p), eccentricity (e_p), and sine inclination ($\sin I_p$), are taken from the AstDys data base (Knežević & Milani 2017). o indicates objects that are stable over the simulated time frame. X shows objects that have at least one particle escaping the population, with their mean respective escape times indicated by colour.

coefficients of determination (R^2) and 1σ errors are presented in Fig. 4. These linear fits are shown in equations (1) for the population, equation (2) for the L_4 swarm, and equation (3) for the L_5. In these equations, the escape percentages (y) are per 1×10^7 yr (x) of the contemporary size of the population (equation 1) and each individual swarms (equations 2–3). These equations are similar, once the bins are taken into account, to those found by Di Sisto et al. (2019), validating our results:

$$y_{pop} = -9.328 \times 10^{-14} x + 0.0007384, \quad (1)$$

$$y_{L4} = -8.581 \times 10^{-14} x + 0.0007085, \quad (2)$$

$$y_{L5} = -1.078 \times 10^{-14} x + 0.000796. \quad (3)$$

Using linear equations (1)–(3), we can calculate the predicted original size of the Jovian population and L_4/L_5 swarms, see Fig. 5, under the assumption that the historical decay of the Trojan population proceeded in the same manner as we see in our simulations. Though the known Jovian Trojan size-frequency distribution, Fig. 2, is only complete to a fraction of the theoretical size, we can still make predictions of the number of objects, placing constraints on their formation and capture. The original population, based on the integration of equation (1), is approximately 1.332 ± 0.004 times the current population. There is an observed difference in the past size of the L_4 and L_5 swarms. Due to the difference in their escape rates, the past L_4 swarm is predicted to be 1.319 ± 0.005 times larger than the contemporary swarm, while the L_5 is 1.358 ± 0.008 times larger. The predicted implantation sizes, based on modern numbers and the escape rates, are 4792 ± 19 for the L_4 and 2606 ± 15 for the L_5. This past ratio reduces the current 1.89 numerical asymmetry to 1.84 ± 0.003. This small difference in past/contemporary size ratio does not account for the modern observed numerical asymmetry, as previously noted (Nesvorný & Dones 2002; Tsiganis et al. 2005b; Di Sisto et al. 2014, 2019).

The *in situ* transport model (Pirani et al. 2019a,b) predicts that the initial mass the Jovian Trojan population was three to four times the magnitude of the observed population. Our escape analysis estimates a primordial population size only 1.332 ± 0.004 times

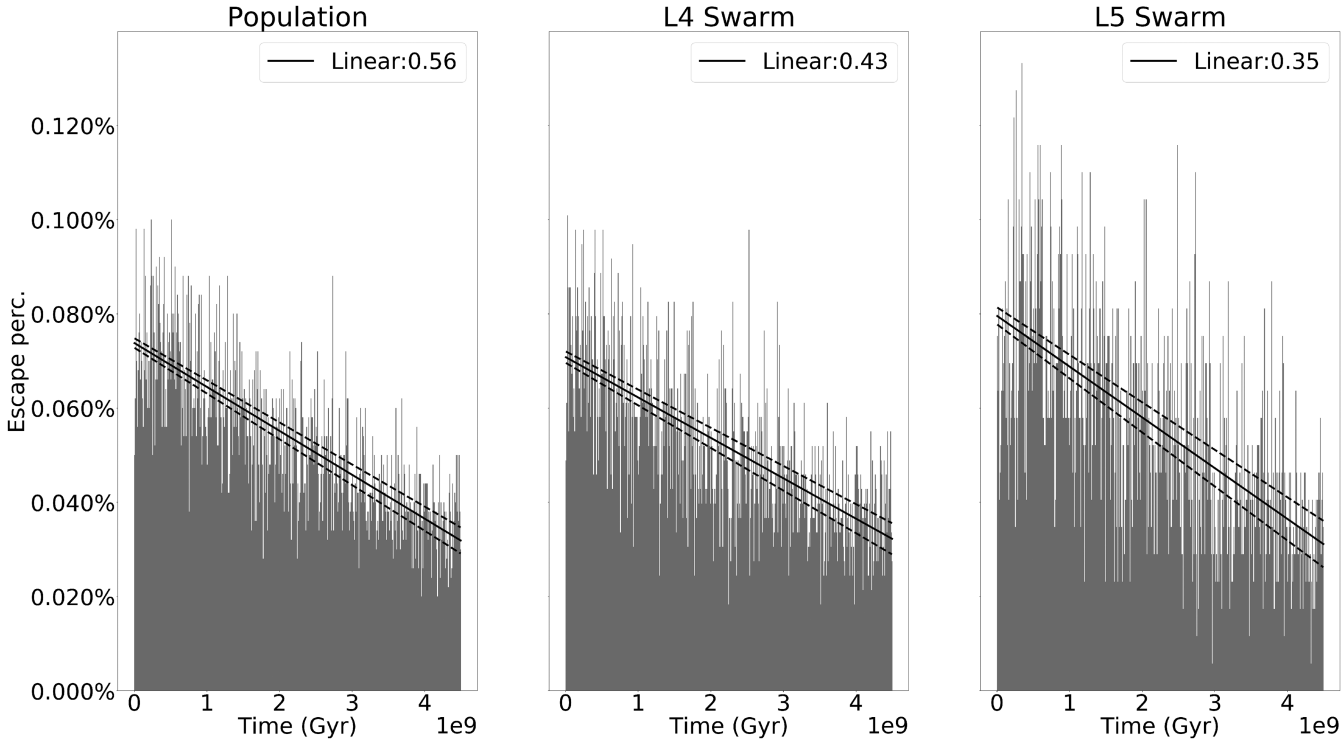

Figure 4. Histograms of escape percentages of the contemporary number, per 1×10^7 yr, of a pool of Jovian Trojan particles, in the combined population, L_4 and L_5 swarms. Lines are linear best fit along with associated R^2 values. Dotted lines are 1σ errors.

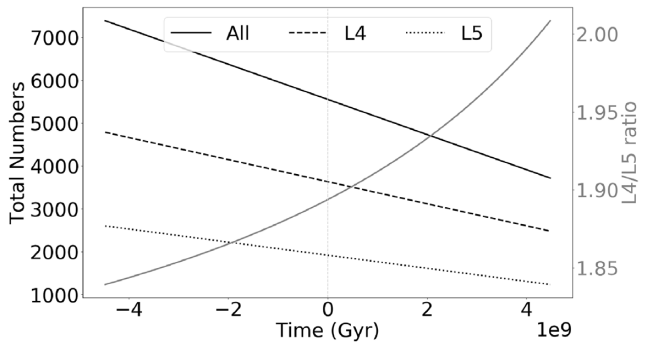

Figure 5. Number of objects, calculated from the contemporary total population (solid line), L_4 (dashed line) and L_5 (dotted line) Jovian Trojan swarms, as a function of time, with 0 time being the present. Right axis shows changing ratio (grey line) between L_4 and L_5 swarms. Plotted from equations discussed in Section 3.1.

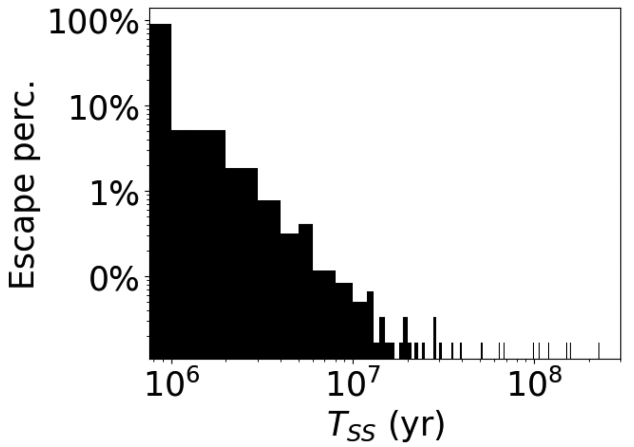

Figure 6. Histogram (1×10^6 yr bins) of time spent in the Solar system prior to ejection (T_{SS}) of objects that escape the Jovian Trojan population. Escape percentages are based of nine particles generated for each of 5553 Jovian Trojans.

larger than today. This is still several orders of magnitude smaller than the most conservative predictions of Pirani et al. (2019a). However, it should be noted that our estimates for the initial population are based on the assumption that the current linear decay has remained consistent since the origin of the Trojan population. In the population's youth, it is possible that the decay rate could have been markedly higher, had objects been efficiently captured to the less stable regions of the Trojan population. Pirani et al. (2019b) do report on interactions with Saturn affecting Trojans larger inclinations, though this is still insufficient to explain the current escape rate.

The majority of escape particles are eventually ejected from the Solar system, by achieving a heliocentric distance of 1000 au, in the same 1×10^5 time-step. This is longer than the expected lifetime of most Centaurs (Horner, Evans & Bailey 2004a), particularly those starting on orbits close to that of Jupiter. A fraction of the population escapees, approximately 41.41 per cent, stay within the Solar system for a longer period of time, prior to being ejected. This fraction is similar between the L_4 and L_5 populations, 41.37 per cent and 41.45 per cent, respectively. This similarity between swarms is not unexpected, since the chaotic evolution of test particles once they leave the Trojan population would be expected to quickly erase any 'memory' of their original orbit. Fig. 6 shows the length of time that these particles spend in the Solar system, with over 88.58 per cent escaping in the first 1×10^6 yr, and an additional

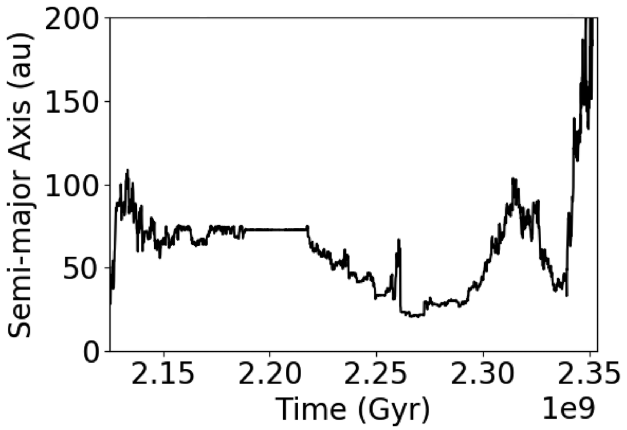

Figure 7. The behaviour of the longest lived escapee, clone 2 of (312627) 2009 TS_{26} in semimajor axis over time. Start time is the point when the particle escapes the L4 Jovian swarm. End time is when the particle escapes the Solar system.

6.15 per cent escaping in the next 1.0×10^6 yr. By 1.0×10^7 yr, 99.25 per cent of the particles have been ejected. These short lifetimes are consistent with the expected lifetimes of Centaurs (Horner et al. 2004a). Horner et al. (2012) show that at least one escaped Jovian Trojan, (1173) Anchises, can participate in the Centaur population before being ejected. Despite this high number of short-lived objects, 13 particles survive longer than 3.2×10^7 yr, the expected lifetime of the longest Centaur (Horner et al. 2004a). These long-lived particles are not unexpected, as Horner et al. (2004a) and Horner, Evans & Bailey (2004b) also reported on several long-lived particles. Each of our clone particles have a different reference object. The longest lived particle is clone 2 of (312627) 2009 TS_{26}, which lives for 2.286×10^8 yr, shown in Fig. 7, and represents a typical chaotic pattern for escaped Trojans.

Less than 10 per cent, 547 objects, of the Jovian Trojan population have been classified under the Bus-Demeo system (Tholen 1984; Bus 2002; Bendjoya et al. 2004; Fornasier et al. 2004, 2007; DeMeo et al. 2009; Carvano et al. 2010; Grav et al. 2012; DeMeo & Carry 2013). The majority, 65.08 per cent, are considered D-types, with several other minor classes X-type (15.17 per cent), C-type (12.79 per cent), and other classes below 5 per cent (P-type, L-type, S-type, V-type, and F-type). The rate at which the three major classes, D-type, X-type, and C-type objects escape, 23.00 per cent, 27.66 per cent, and 24.13 per cent, respectively, is roughly constant with the overall population. Many of the smaller taxonomic classes come from Carvano et al. (2010), Hasselmann, Carvano & Lazzaro (2012), and have low classification confidence levels. If we reduce the taxonomic data set to only those in Carvano et al. (2010) and Hasselmann et al. (2012) with a confidence classification of greater than 50, it reduces the classified Trojans down to 2 per cent of the population, and only D-type (79.24 per cent), X-type (14.15 per cent), and C-type (6.6 per cent) objects. This restriction does not change the escape rates significantly for the D-types at 23.41 per cent. The X-types and C-types do increase to 32.59 per cent and 31.75 per cent, respectively, though these classes suffer from the variances of small number statistics. This classification analysis is something that may merit further study once data becomes available from the Rubin Observatory LSST (Schwamb et al. 2018a,b), and our escape analysis can then be placed in a wider taxonomic context.

4 COLLISIONAL FAMILIES

In order to further investigate the escapes of collisional family members, we have increased the number of clones simulated to 125 for each of the canonical family members in Nesvorný et al. (2015). This increases the statistical significance of the escape analysis. For comparison purposes, the wider, non-canonical family data sets found by Brož & Rozehnal (2011) and Rozehnal et al. (2016) use the original eight clones, as in Section 3, and only those objects found in the AstDys data base (Knežević & Milani 2017).

The specific numbers of canonical collisional family members that are simulated in this work are shown in Table 3, after Nesvorný et al. (2015). Of particular interest is the Eurybates family. This is the largest known family in the Jovian Trojan population and is discussed separately in Section 4.1.1. When all of the particles are considered independently, f_{EscP} and f_{VEscP} in Table 3, the percentage that escape is similar to the escape rate of the reference particles (f_{EscR} and f_{VEscR} in Table 3). This is comparable to the trends seen in the overall swarms (see Section 3).

In general terms, the members of known collisional families within our integrations show lower escape percentages than the total of the swarms. This is due to the fact that the majority of the known collisional families are located in the more stable regions of the delta semimajor axis, eccentricity, and sin i parameter space, as discussed in Sections 4.1 and 4.2.

There are also potentially a significant number of undetected family members (Yoshida & Nakamura 2008; Vinogradova & Chernetenko 2015) in the Jovian Trojan population. The numerical escape percentages may increase as a larger number of objects are discovered by new surveys, such as the Rubin Observatory LSST (Schwamb et al. 2018a), which is expected to commence science operations in 2023. As these new objects are discovered, their allocation to collisional families and long-term stabilities will need to be investigated.

4.1 L4 collisional Families

In the L_4 swarm, shown in Fig. 8, a total four families have been identified. The largest L_4 cluster, the Eurybates family is discussed in Section 4.1.1.

4.1.1 Eurybates family

The Eurybates family is the largest and most consistently identified (Brož & Rozehnal 2011; Nesvorný et al. 2015; Vinogradova 2015) collisional cluster in the Trojan population. The largest fragment of the family, (5348) Eurybates, is also the target of future visitation by the *Lucy* spacecraft in 2027 (Levison et al. 2017). In our simulations, we consider the canonical 218 identified members of the family (Nesvorný et al. 2015). From the 310 members identified by Brož & Rozehnal (2011), 293 are in the AstDys data base. In the canconcial members, there is a 19.59 per cent escape percentage for the particle pool. If we consider the larger set identified by Brož & Rozehnal (2011), this escape percentage only decreases slightly to 19.07 per cent.

As was seen in the L_4 swarm (Fig. 3), there is a gradient to the escape from the Eurybates family (Fig. 9) with larger changes in semimajor axis (Δa_p) and eccentricity (e_p), causing particles to escape the swarm sooner. Contrary to the overall decreasing escape rates seen in the L_4 swarm, we found the escape rate of the Eurybatyes family to be increasing with time, as can be seen in Fig. 10. A possible explanation for this is the ongoing diffusion of

Table 3. Escaping collisional family members; n: number of objects in each canonical collisional family (Nesvorný et al. 2015); the n_{EscR}: number of reference particles that escape: f_{EscR}: numerical percentage of reference particles that escape; f_{VEscR}: volumetric percentage of reference particles that escape; f_{EscP}: numerical percentage Trojan particle pool, Reference and 125 1σ clones, that escape; f_{VEscP}: volumetric percentage Trojan particle pool, Reference and 125 1σ clones, that escape.

	n	n_{EscR}	f_{EscR} (per cent)	f_{VEscR} (per cent)	f_{EscP} (per cent)	f_{VEscP} (per cent)
L_4 Families						
Eurybates (1)	218	43	19.72	7.43	19.59	8.05
Hektor (2)	12	2	16.66	0.06	11.99	28.53
1996 RJ (3)	7	0	0.00	0.00	0.00	0.00
Arkesilaos (4)	37	1	2.70	1.13	3.09	3.47
L_5 Families						
Ennomos (5)	30	15	50.00	66.39	34.29	17.47
2001 UV_{209} (6)	13	0	0.00	0.00	0.00	0.00
Total	317	61	19.24	12.45	17.67	24.75%

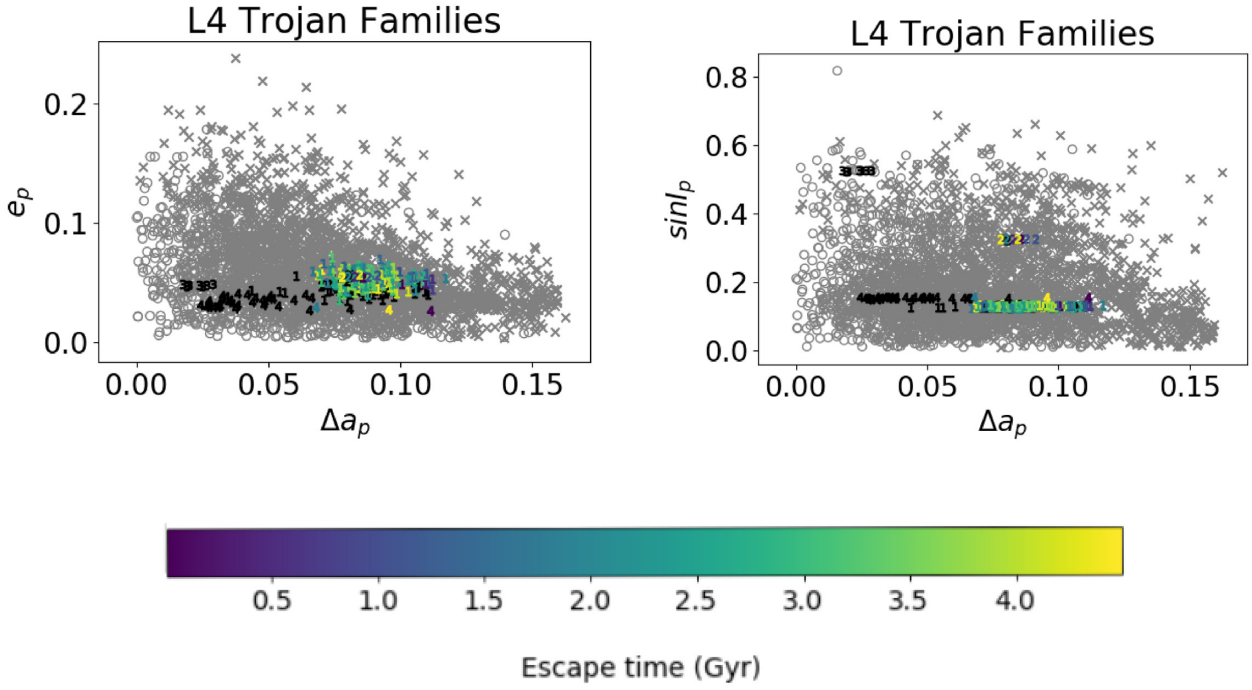

Figure 8. Escape analysis of collisional family members located in the L_4 Jovian Trojan swarm simulated for 4.5×10^9 yr. Shown are the instabilities of the reference object. Proper elements, semimajor axis (Δa_p), eccentricity (e_p), and sine inclination ($\sin I_p$), are taken from the AstDys data base (Knežević & Milani 2017). o indicates objects that are stable over the simulated time frame. x are unstable background objects. Family membership: Eurybates (1), Hektor (2), 1996 RJ (3), Arkesilaos (4). Black numbers are stable, with colours showing mean particle escape time.

family members into less stable parameter space, as they disperse chaotically from the initial location of the breakup event. Such dispersion can be seen in main belt families (Milani & Knežević 1992; Bottke et al. 2005; Brož & Morbidelli 2013; Aljbaae et al. 2019), with members gradually diffusing into Jovian resonances and being ejected from the main belt. Future simulations of a synthetic Eurybates family would be required to confirm this, and are beyond the scope of this paper.

As with the L_4 swarm escape analysis, a standard linear regression offers the most reliable fit for the data. We did attempt to create a second-order polynomial, along with using cumulative linear and polynomial regression to improve the fit in this case, though as Fig. 10 demonstrates, this did not improve the coefficient of determination. The coefficient of determination for the linear fit ($R^2 = 0.42$) is similar to the L_4 swarm, due to number of particles being considered being an order of magnitude smaller. We attempted to take account for this by using an order of magnitude larger bins to increase the number of ejections per bin to a reasonable number. The y-intercept of this linear equation, which represents the time at which the escape rate from the Eurybates family equals zero, might be considered to be an indication of the age of the family. If such a conclusion is reasonable, our data would place the family formation event some $1.045 \pm 0.364 \times 10^9$ yr ago. This age is presented as a minimum age, though preliminary simulations of a synthetic Eurybates family (Holt et al. 2019) indicate that the observed dynamical situation could be achieved within 1×10^5 yr.

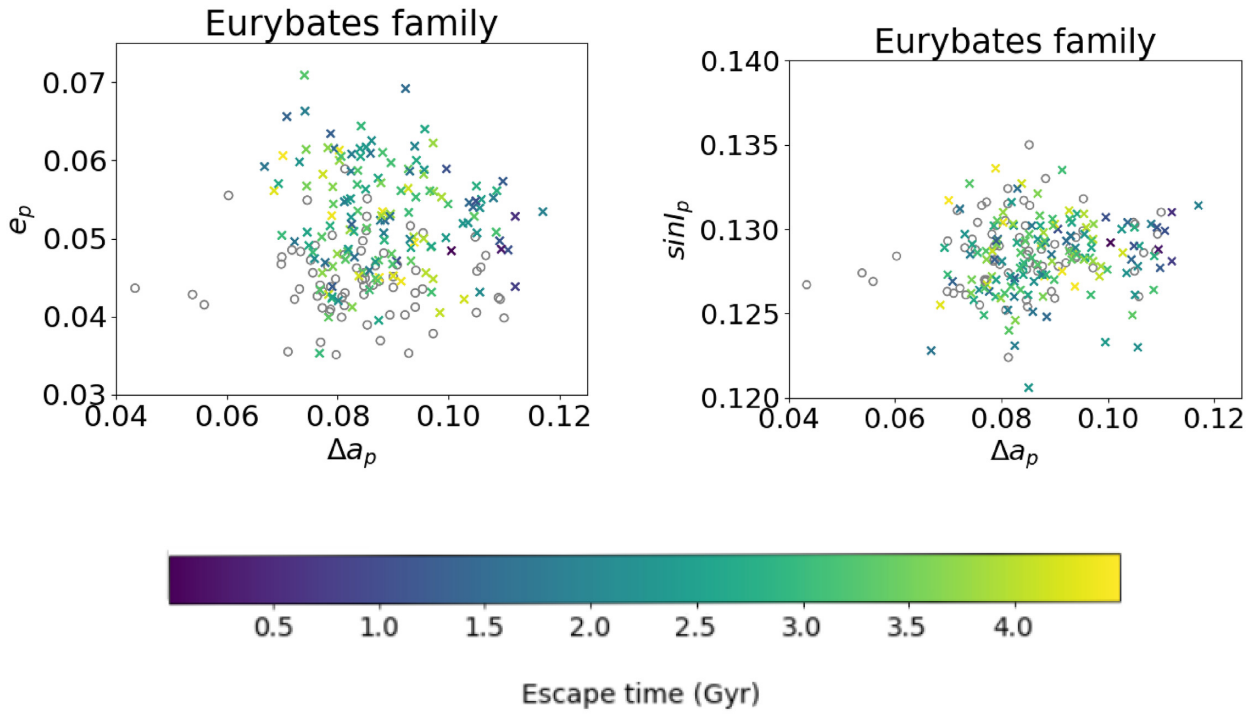

Figure 9. Escape analysis of the canonical Eurybates collisional family members identified in Nesvorný et al. (2015), simulated for 4.5×10^9 yr. Shown are the mean escape time of 126 particles for the object (coloured x). Proper elements, semimajor axis (Δa_p), eccentricity (e_p), and sine inclination ($\sin I_p$) are taken from the AstDys data base (Knežević & Milani 2017). o indicates objects that are stable over the simulated time frame.

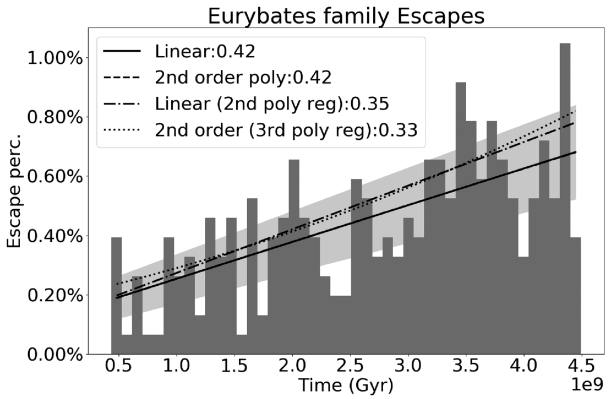

Figure 10. Histogram (1×10^8 yr bins) of escapes from the Eurybates collisional family. Lines indicate best-fitting analysis scaled to the histogram bins, with R^2 scores for linear fit (solid, with light grey shading indicating 1σ error) and second degree polynomial (dashed) lines. Fits are also shown from the results of linear regression analysis on second (dot–dashed) and third-order polynomial (doted) generated from a cumulative histogram.

As previously stated, the two other methods of collisional family age estimation, high precision reverse integration (Nesvorný et al. 2002a) and Yarkvosky 'V' (Milani et al. 2017) are inappropriate for the Trojan families. Using a small number of synthetic members, Brož & Rozehnal (2011) also calculated a wide time range, 1–4Gyr, for the family creation event. Our age is therefore one of the first estimations that give a reasonable order of magnitude age and constrained range for the Eurybates family. As larger numbers of family members are identified, a re-investigation should improve the statistical reliability of this analysis.

4.1.2 *Hektor family*

Rozehnal et al. (2016) identified 90 objects in this family, using the Random box method. We use the canonical 12 objects from Nesvorný et al. (2015), and note where there could possibly be a different escape rate. The family is characterized by a moderate Δa_p and e_p, with a comparatively high $\sin I_p$. The parent body, (624) Hektor has been classified under the Bus-Demeo spectral taxonomy (DeMeo et al. 2009) as a D-type asteroid (Emery, Cruikshank & Van Cleve 2006; Emery, Burr & Cruikshank 2011; Rozehnal et al. 2016). It is also a contact binary, with a confirmed satellite (Marchis et al. 2014). The canonical Hektor family has a low escape rate, with only two reference particles from the family eventually escaping the swarm. One of these is the reference particle of (624) Hektor itself, which also has a 28.8 per cent particle escape rate. These particles account for the large volume of escapes, nearly double that of the numerical escape fraction. Unfortunately, the small number of identified members of the Hektor family, 12 known objects, means that a statistical analysis of these results would prove problematic. Using the larger number of clones, we can assign a numerical escape percentage of 12 per cent. If the wider numbers, 77 objects from Rozehnal et al. (2016) are used, then 18.18 per cent of particles escape.

4.1.3 *1996 RJ family*

The compact 1996 RJ family has a small Δa_p and e_p. This places it firmly within the predicted stability region from Nesvorný & Dones (2002). The high inclinations of the family members do not seem to have an effect on their stability. Our results show that this family is completely stable, with no escapes. Those members from Rozehnal et al. (2016) are also stable, except for the single particle, clone 6 of

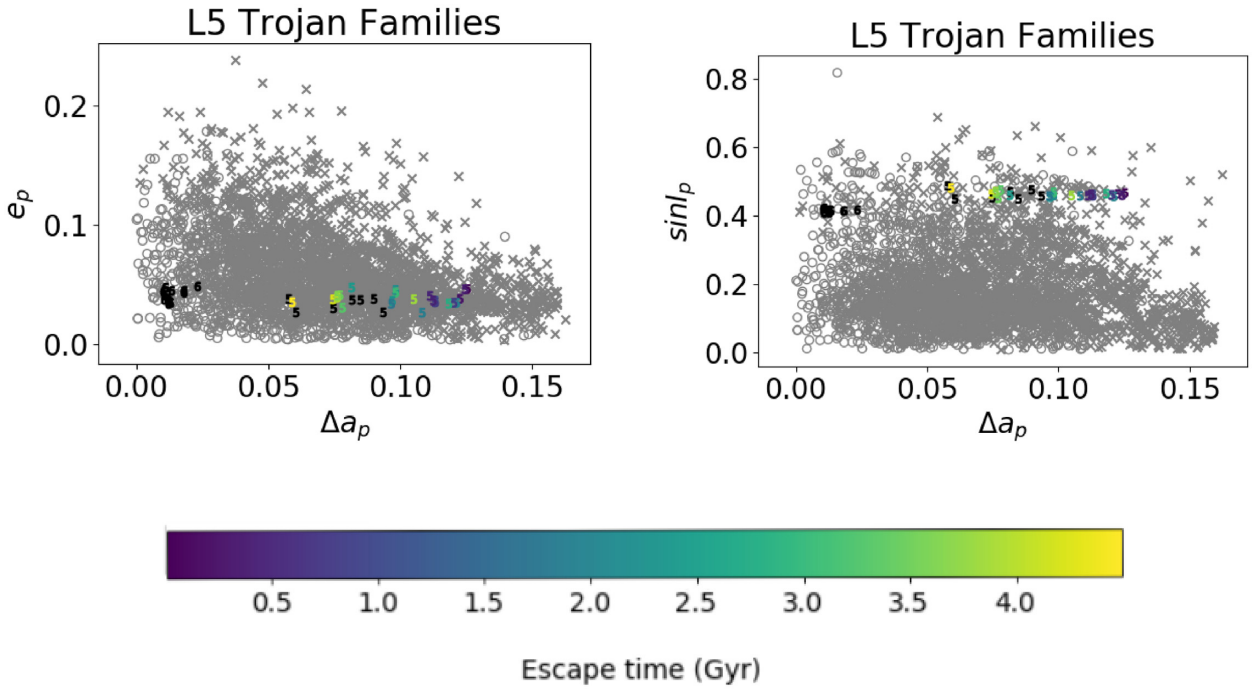

Figure 11. Escape analysis of collisional family members located in the L_5 Jovian Trojan Swarm simulated for 4.5e9 yr. Proper elements, delta semimajor axis (Δa_p), eccentricity (e_p), and sine inclination (sinI_p), are taken from the AstDys data base (Knežević & Milani 2017). o indicates objects that are stable over the simulated time frame. x are unstable background objects. Numbers indicate collisional family membership: Ennomos (5), 2001 UV_{209} (6). Black numbers are stable, with colours showing mean escape time of 126 particles for the object.

(195104) 2002 CN_{130}. This particular object has a higher Δa_p than the rest of the family, and is a probable outlier.

4.1.4 Arkesilaos family

This is a medium-sized family, with 37 cannonical members. It is confirmed by Vinogradova (2015), though they use (2148) Epeios as the main object and have a larger number of members (130). Rozehnal et al. (2016) chose (20961) Arkesilaos as the primary objects due to consistency at the centre of the family parameter space, even at low cut-off velocities. The family has a wide distribution of Δa_p values and a compact range of e_p and sinI_p values. Predictably, the family is stable with three small outliers that escape. (356237) 2009 $SA_3 28$ is the most unstable, with 72 per cent of the particles escaping. This is due to its high Δa_p, placing it in the unstable parameter space. (394808) 2008 RV_{124} and (20961) Arkesilaos also have some particles escape, but only 28.9 per cent and 14.4 per cent, respectively. The escape fraction of the family only changes slightly to 2.24 per cent, considering the additional members identified by Rozehnal et al. (2016). The small escape percentages of this family preclude any additional statistical analysis.

4.2 L5 Collisional families

Within the L5 swarm, there are only two identified collisional families (Nesvorný et al. 2015), the Ennomos and 2001 UV_{209} families. Contrary to Rozehnal et al. (2016) and the canonical Nesvorný et al. (2015), Vinogradova (2015) do not consider either of the families valid, though they note that there is some clustering around the largest members. We show the escape times of the L5 families in Fig. 11.

4.2.1 Ennomos family

The most unstable cluster in the L5 swarm is the Ennomos family. This is a medium-sized cluster, with 30 identified objects in Nesvorný et al. (2015). There are a larger number of objects, 104, of which 85 are in the Astdys data base, identified by Rozehnal et al. (2016). The family members have relatively high Δa_p and sinI_P, with low e, placing them on the edge of the stable parameter space. Consequently, a large fraction of Ennomos family members, 50 per cent of reference particles, escape the swarm. When considering just the reference particles, 66.66 per cent of the volume escape during our simulations. This is due to the reference particle and a low number of clones (14.28 per cent) of (1867) Deiphobus, a 59 km object, escaping the L_5 swarm. In the more statistically robust particle pool, the escape percentage by volume drops to 17.47 per cent. This family is characterized by its high inclination and delta semimajor axis, so a high amount of instability is not unexpected. In this family, there are three members, (48373) Gorgythion, (381987) 2010 HZ_{21} and (287454) 2002 YX_7 where all particles escape. This is unsurprising, as (48373) Gorgythion has the largest proper Δa_p and e_p of the family. In addition to these three, six objects have over 50 per cent of their particles escape. Including the larger number of members from Rozehnal et al. (2016), decreases the escape rate to 23.14 per cent, closer to the overall L5 rate.

As in Section 4.1.1, we attempted regression analysis to ascertain the age of this family. Brož & Rozehnal (2011) estimate the age of the family to be approximately 1–2 Gya. Similar to the L5 swarm and unlike the Eurybates family, the slope of the linear regression analysis is negative, though fairly flat (-1.62×10^{-12}). The R^2 score is only 0.13, so until additional family members are identified, these are only preliminary indications.

4.2.2 2001 UV_{209}

This small family, with thirteen canonical members, is located well within the stable Δa_p–e parameter space. It is then not unexpected that the 2001 UV_{209} family members are stable in our simulations. Considering the expanded 36 objects identified by Rozehnal et al. (2016), this jumps to 13.89 per cent. These unstable members are not considered valid by Nesvorný et al. (2015), and with higher Δa_p are probable background objects, rather than members of the family.

5 CONCLUSIONS

The Jovian Trojans are a fascinating collection of objects, remnants of the early stages of the Solar system's formation. In this work, we present the results of detailed *n*-body simulations of the known Jovian Trojan population, using nearly double the number of objects of the previous largest study (Di Sisto et al. 2014, 2019). We simulate the orbital evolution of a population of 49 977 massless test particles, nine particles for each of the 5553 known Jovian Trojans, for a period of 4.5×10^9 yr into the future, under the gravitational influence of the Sun and the four giant planets. Our simulations reveal that the populations of both the L_4 and L_5 swarms are predominately stable; however, a significant number of objects from both swarms can escape over the lifetime of the Solar system. In the case of the leading L_4 swarm, we find that 23.35 per cent of objects escape, by volume. Similarly, only 24.89 per cent escape the trailing L_5 swarm. Overall, 23.95 per cent by volume of all test particles simulated in this work escape the Jovian population. As discussed by other authors (Nesvorný & Dones 2002; Tsiganis et al. 2005b; Nesvorný et al. 2013; Di Sisto et al. 2014, 2019), we find that the escape rates cannot explain the current observed asymmetry between the two swarms. This supports the conclusion that the observed asymmetry between the L_4 and L_5 swarms are the result of their initial capture implantation (Nesvorný et al. 2013; Pirani et al. 2019a).

The escape rates of objects from the two Trojan swarms are in accordance with the idea that the Jovian Trojans act as a source of material to the other small Solar system body populations, as noted in Levison et al. (1997), Di Sisto et al. (2014), Di Sisto et al. (2019), particularly with regards to the Centaurs (Horner et al. 2004a, 2012). The majority of escaped Trojans, 58.63 per cent, are ejected from the population and the Solar system within a single 1×10^5 yr time-step. For those that remain in the Solar system, 99.25 per cent are ejected by 1×10^7 yr, after joining the Centaur population.

In the Jovian Trojan swarms, a total of six collisional families have been identified to date (Nesvorný et al. 2015), with four in the L_4 swarm and two located around L_5. We find that three of the families are highly dynamically stable, with no particles escaping the Trojan population through the course of our integrations (the 1996 RJ, Arkesilaos and 2001 UV_{209} families). Two other collisional groups, the L4 Hektor and L5 Ennomos families did have members that escape. These unstable families all have a small number of known members, which limits our ability to study their stability further in this work. The largest known Trojan family, the Eurybates L4 family, has a smaller escape rate than the overall population. Contrary to the escape trends in the population, however, the escape rate of the Eurybates family is found to increase with time in our simulations. This might point to the diffusion of its members into unstable parameter space as they evolve away from the location of the family's creation. From this escape rate, we can obtain an estimate of the age of the Eurybates family on the order of $1.045 \pm 0.364 \times 10^9$ yr.

In the future, as more members of the Jovian Trojans and their taxonomic groupings are identified, it will be interesting to see whether these dynamical methods can be used to help constrain the ages of the smaller clusters. If this is possible, such results would shed light on the variability of the collision rates within the Jovian Trojan swarms. The results we present in this paper, and these potential future works, highlight the impotence of the Jovian Trojan swarms, their taxonomic groups and collisional families, to understanding the history of the Solar system.

ACKNOWLEDGEMENTS

This research was in part supported by the University of Southern Queensland's Strategic Research Initiative programme. TRH was supported by the Australian Government Research Training Program Scholarship. This work makes use of the Anaconda Python software environment (Continuum Analytics 2016). We thank Hal Levison for discussions on the paper and for providing previously unpublished data. We also thank Douglas Hamilton and Romina Di Sisto (as a reviewer) for providing comments and insights on this paper. This research has made use of NASA Astrophysics Data System Bibliographic Services.

REFERENCES

Aljbaae S., Souchay J., Prado A. F. B. A., Chanut T. G. G., 2019, A&A, 622, A39
Barnes R., Quinn T. R., 2004, AJ, 611, 494
Beaugé C., 2001, Icarus, 153, 391
Bendjoya P., Cellino A., Di Martino M., Saba L., 2004, Icarus, 168, 374
Bolin B. T., Delbó M., Morbidelli A., Walsh K. J., 2017, Icarus, 282, 290
Bottke W. F., Durda D. D., Nesvorný D., Jedicke R., Morbidelli A., Vokrouhlický D., Levison H. F., 2005, Icarus, 179, 63
Bottke W. F., Vokrouhlický D., Rubincam D., Nesvorný D., 2006, Ann. Rev. Earth Planet. Sci., 34, 157
Bottke W. F., Nesvorný D., Vokrouhlický D., Morbidelli A., 2010, AJ, 139, 994
Brown M. E., Barkume K. M., Ragozzine D., Schaller E. L., 2007, Nature, 446, 294
Brož M., Morbidelli A., 2013, Icarus, 223, 844
Brož M., Rozehnal J., 2011, MNRAS, 414, 565
Brož M., Vokrouhlický D., 2008, MNRAS, 390, 715
Brož M., Vokrouhlický D., Roig F., Nesvorný D., Bottke W. F., Morbidelli A., 2005, MNRAS, 359, 1437
Bus S. J., 2002, Icarus, 158, 146
Carruba V., Domingos R. C., Nesvorný D., Roig F., Huaman M. E., Souami D., 2013, MNRAS, 433, 2075
Carvano J. M., Hasselmann P. H., Lazzaro D., Mothé-Diniz T., 2010, A&A, 510, A43
Continuum Analytics, 2016, Anaconda Software Distribution. Version 2.4.0. Available at: https://continuum.io
de la Fuente Marcos C., de la Fuente Marcos R., 2018, MNRAS, 474, 838
De Luise F., Dotto E., Fornasier S., Barucci M. M. A., Pinilla-Alonso N., Perna D., Marzari F., 2010, Icarus, 209, 586
Deienno R., Morbidelli A., Gomes R. S., Nesvorný D., 2017, AJ, 153, 153
Delbó M., Walsh K., Bolin B., Avdellidou C., Morbidelli A., 2017, Science, 357, 1026
DeMeo F. E., Carry B., 2013, Icarus, 226, 723
DeMeo F. E., Binzel R. P., Slivan S. M., Bus S. J., 2009, Icarus, 202, 160
Di Sisto R. P., Ramos X. S., Beaugé C., 2014, Icarus, 243, 287
Di Sisto R. P., Ramos X. S., Gallardo T., 2019, Icarus, 319, 828
Ebell M., 1909, Astron. Nachr., 180, 213
Emery J. P., Cruikshank D. P., Van Cleve J., 2006, Icarus, 182, 496
Emery J. P., Burr D. M., Cruikshank D. P., 2011, AJ, 141, 25

Emery J. P.,Marzari F., Morbidelli A., French L. M., Grav T., 2015, in Michel P., DeMeo F., Bottke W., eds, Asteroids IV. Univ. Arizona Press, Tucson, AZ, p. 203
Fernández Y. R., Jewitt D., Ziffer J. E., 2009, AJ, 138, 240
Fornasier S., Dotto E., Marzari F., Barucci M., Boehnhardt H., Hainaut O., Debergh C., 2004, Icarus, 172, 221
Fornasier S., Dotto E., Hainaut O., Marzari F., Boehnhardt H., Deluise F., Barucci M., 2007, Icarus, 190, 622
Giorgini J. D. et al., 1996, American Astronomical Society, DPS meeting #28, id.25.04
Gradie J. C., Chapman C. R., Williams J. G., Gradie J. C., Chapman C. R., Williams J. G., 1979, in Gehrels T., ed., Asteroids. Univ. Arizona Press, Tucson, AZ, p. 359
Grav T., Bauer J. M., 2007, Icarus, 191, 267
Grav T., Holman M. J., Gladman B. J., Aksnes K., 2003, Icarus, 166, 33
Grav T. et al., 2011, Astrophys. J., 742, 40
Grav T., Mainzer A. K., Bauer J. M., Masiero J. R., Nugent C. R., 2012, Astrophys. J., 759, 49
Harris A. W., 1997, Icarus, 126, 450
Hasselmann P. H., Carvano J. M., Lazzaro D., 2012, NASA Planetary Data System. Available at: https://pds.nasa.gov/ds-view/pds/viewDataset.jsp?dsid=EAR-A-I0035-5-SDSSTAX-V1.1
Heinrich V., 1907, Astron. Nachr., 176, 193
Hellmich S., Mottola S., Hahn G., Kührt E., de Niem D., 2019, A&A, 630, A148
Hirayama K., 1918, AJ, 31, 185
Holt T. R., Brown A. J., Nesvorný D., Horner J., Carter B., 2018, ApJ, 859, 97
Holt T., Nesvorny D., Horner J., King R., Carter B., Brookshaw L., 2019, AAS Division on Dynamical Astronomy Meeting #50, id. 100.01
Homer, 750 BC, The Iliad & The Odyssey, 2013 edn. Barnes & Noble, New York, NY
Horner J., Evans N. W., Bailey M. E., 2004a, MNRAS, 354, 798
Horner J., Evans N. W., Bailey M. E., 2004b, MNRAS, 355, 321
Horner J., Müller T. G., Lykawka P. S., 2012, MNRAS, 423, 2587
Jewitt D. C., 2018, AJ, 155, 56
Jewitt D. C., Haghighipour N., 2007, ARA&A, 45, 261
Jewitt D. C., Trujillo C. A., Luu J. X., 2000, AJ, 120, 1140
Knežević Z., Milani A., 2003, A&A, 403, 1165
Knežević Z., Milani A., 2017, AstDys: Synthetic Proper Elements 5553 Numbered and Multiopposition Trojans. Available at: https://newton.spacedys.com/~astdys2/propsynth/tro.syn
Kopff A., 1909, Astron. Nachr., 182, 25
Lagrange J.-L., 1772, Prix de l'académie Royale des Sciences de Paris, 9, 292
Levison H. F., Shoemaker E. M., Shoemaker C. S., 1997, Nature, 385, 42
Levison H. F., Morbidelli A., Vokrouhlický D., Bottke W. F., 2008, AJ, 136, 1079
Levison H. F., Morbidelli A., Tsiganis K., Nesvorný D., Gomes R., 2011, AJ, 142, 152
Levison H. F., Olkin C. B., Noll K., Marchi S., Lucy Team, 2017, 48th Lunar and Planetary Science Conference, held 20–24 March 2017, at The Woodlands, Texas, ID: 2025
Lykawka P. S., Horner J., 2010, MNRAS, 405, 1375
Marchis F. et al., 2006, Nature, 439, 565
Marchis F. et al., 2014, Astrophys. J., 783, L37
Milani A., 1993, Celst. Mech. Dyn. Astron., 57, 59
Milani A., Farinella P., 1994, Nature, 370, 40
Milani A., Knežević Z., 1992, Icarus, 98, 211
Milani A., Knežević Z., Novaković B., Cellino A., 2010, Icarus, 207, 769
Milani A., Cellino A., Knežević Z., Novaković B., Spoto F., Paolicchi P., 2014, Icarus, 239, 46
Milani A., Knežević Z., Spoto F., Cellino A., Novaković B., Tsirvoulis G., 2017, Icarus, 288, 240
Morbidelli A., 2010, Comptes Rendus Physique, 11, 651
Morbidelli A., Levison H. F., Tsiganis K., Gomes R., 2005, Nature, 435, 462
Nakamura T., Yoshida F., 2008, PASJ, 60, 293
Nesvorný D., 2018, ARA&A, 56, 137
Nesvorný D., Dones L., 2002, Icarus, 160, 271
Nesvorný D., Morbidelli A., 2012, AJ, 144, 117
Nesvorný D., Bottke W. F., Dones L., Levison H. F., 2002a, Nature, 417, 720
Nesvorný D., Morbidelli A., Vokrouhlický D., Bottke W. F., Brož M., 2002b, Icarus, 157, 155
Nesvorný D., Thomas F., Ferraz-Mello S., Morbidelli A., 2002c, Celest. Mech. Dyn. Astron., 82, 323
Nesvorný D., Alvarellos J. L. A., Dones L., Levison H. F., 2003, AJ, 126, 398
Nesvorný D., Beaug C., Dones L., 2004, AJ, 127, 1768
Nesvorný D., Vokrouhlický D., Morbidelli A., 2013, ApJ, 768, 45
Nesvorný D., Brož M., Carruba V., 2015, in Michel P., DeMeo F. E., Bottke W. F., eds, Asteroids IV. Univ. Arizona Press, Tucson, AZ, p. 297
Paolicchi P., Spoto F., Knežević Z., Milani A., 2019, MNRAS, 484, 1815
Pirani S., Johansen A., Bitsch B., Mustill A. J., Turrini D., 2019a, A&A, 623, A169
Pirani S., Johansen A., Mustill A. J., 2019b, A&A, 631, A89
Rein H., Liu S.-F., 2012, A&A, 537, A128
Rein H., Tamayo D., 2015, MNRAS, 452, 376
Roig F., Ribeiro A. O., Gil-Hutton R., 2008, A&A, 483, 911
Romanishin W., Tegler S. C., 2018, AJ, 156, 19
Rozehnal J., Brož M., Nesvorný D., Durda D. D., Walsh K. J., Richardson D. C., Asphaug E., 2016, MNRAS, 462, 2319
Schwamb M. E. et al., 2018a, preprint (arXiv:1802.01783)
Schwamb M. E., Levison H. F., Buie M. W., 2018b, Res. Notes AAS, 2, 159
Sharkey B. N. L., Reddy V., Sanchez J. A., Izawa M. R. M., Emery J. P., 2019, AJ, 158, 204
Sheppard S. S., Jewitt D. C., 2003, Nature, 423, 261
Šidlichovský M., Nesvorný D., 1996, Celest. Mech. Dyn. Astron., 65, 137
Slyusarev I. G., Belskaya I. N., 2014, SoSyR, 48, 139
Spoto F., Milani A., Knežević Z., 2015, Icarus, 257, 275
Strömgren E., 1908, Astron. Nachr., 177, 123
Tholen D. J., 1984, PhD thesis, Univ. Arizona, Tucson
Tsiganis K., Gomes R., Morbidelli A., Levison H. F., 2005a, Nature, 435, 459
Tsiganis K., Varvoglis H., Dvorak R., 2005b, Celest. Mech. Dyn. Astron., 92, 71
Turrini D., Marzari F., Beust H., 2008, MNRAS, 391, 1029
Turrini D., Marzari F., Tosi F., 2009, MNRAS, 392, 455
Vinogradova T. A., 2015, MNRAS, 454, 2436
Vinogradova T. A., Chernetenko Y. A., 2015, Solar Syst. Res., 49, 391
Vokrouhlický D., Brož M., Bottke W. F., Nesvorný D., Morbidelli A., 2006, Icarus, 182, 118
Wang X., Hou X., 2017, MNRAS, 471, 243
Warner B. D., Harris A. W., Vokrouhlický D., Nesvorný D., Bottke W. F., 2009, Icarus, 204, 172
Wolf M., 1907, Astron. Nachr., 174, 47
Wong I., Brown M. E., 2016, AJ, 152, 90
Yoshida F., Nakamura T., 2008, Publ. Astron. Soc. Japan, 60, 297
Yoshida F., Terai T., 2017, AJ, 154, 71
Zappala V., Farinella P., Knežević Z., Paolicchi P., 1984, Icarus, 59, 261
Zappala V., Cellino A., Farinella P., Knežević Z., 1990, AJ, 100, 2030
Zappala V., Cellino A., Farinella P., Milani A., 1994, AJ, 107, 772

SUPPORTING INFORMATION

Supplementary data are available at *MNRAS* online.

Holtetal2020_JovTrojanEscapes.csv

Please note: Oxford University Press is not responsible for the content or functionality of any supporting materials supplied by the authors. Any queries (other than missing material) should be directed to the corresponding author for the article.

This paper has been typeset from a TEX/LATEX file prepared by the author.